International Congress Series 1281 (2005) 351–356

www.ics-elsevier.com

Automatic cardiac contour propagation in short axis cardiac MR images

G.L.T.F. Hautvast[a,b,*], M. Breeuwer[a], S. Lobregt[a], A. Vilanova[b], F.A. Gerritsen[a,b]

[a]*Medical IT Advanced Development-Philips Medical Systems, Best, The Netherlands*
[b]*Biomedical Imaging and Modeling-Technische Universiteit Eindhoven, The Netherlands*

Abstract. Active contours are a popular method for automatic extraction of object boundaries based on image features in medical images. However, in short axis cardiac MR images, they fail to give correct results due to the presence of papillary muscles along the left ventricular endocardium boundary. We propose a new automatic cardiac contour propagation method based on active contours. The method can be used to propagate cardiac contours that conform an initial manual segmentation, by exploiting information in adjacent images. In this paper, we present the results of the optimization and extensive validation of our method, which was found to be robust and accurate for the delineation of the LV endocardium, LV epicardium and RV endocardium contours. Additionally, the processing time is reduced significantly compared with manual contour delineation.

Keywords: Active contour; Cardiac segmentation; Propagation

1. Introduction

Short axis cine cardiac MRI acquisitions usually consist of 15–25 phases at 10–15 slices (150–375 images) that are approximately perpendicular to the long axis of the left ventricle. Segmentation of the left ventricular (LV) and right ventricular (RV) blood pool and the myocardium is required for quantification and diagnosis of cardiac function. Current automatic segmentation methods often do not provide adequate contours in the

* Corresponding author. Biomedical Imaging and Modeling-Technische Universiteit Eindhoven, The Netherlands.
E-mail address: gilion.hautvast@philips.com (G.L.T.F. Hautvast).

0531-5131/
doi:10.1016/j.ics.2005.03.267

presence of papillary muscles or trabeculae, requiring elaborate interaction of a skilled user. Besides this, currently applied automatic methods often make little or no use of anatomical knowledge and of already defined contours in adjacent images.

2. Purpose

The purpose of our work is to reduce user interaction to drawing a single initial segmentation by developing a dedicated contour propagation method based on Active Contours [1]. The method propagates contours over all phases exploiting information from adjacent images, to generate contours reflecting the preferences of the user (e.g. inclusion or exclusion of the papillary muscles).

3. Methods

3.1. Active contours

The starting point for the new method was the Active Contour [1], currently used in the Philips Medical Systems ViewForum workstation (formerly EasyVision). The structure of this contour model is a set of connected vertices. The movement of these vertices is limited to the direction perpendicular to the contour. The internal forces in this algorithm minimize the curvature of the contour. These internal forces are balanced with external forces, to define a total force for each vertex, which drives the contour to its final location. For our purpose, the external force is redefined to use information from adjacent images by applying gray value profile matching.

3.2. Profile matching

To imitate the initial segmentation, the vertices of the contour should be driven to locations with a similar gray value neighborhood. This gray value neighborhood can be represented by profiles perpendicular to the contour. Features in these profiles, such as the transition between blood and myocardium, are translated between phases due to the contracting motion of the heart. We calculate an external energy distribution by calculating the match between profiles in the reference and the target phase. The resulting distribution has a well-defined minimum at the location where the target profile is translated such that it best resembles the reference profile (see Fig. 1). This is accomplished by calculating normalized sums of differences between reference and translated target profiles. This external energy distribution drives the Active Contour towards locations with similar contour neighborhoods. By repeating this process from phase to phase, the ‘initial behavior’ of the contour is copied, until each phase in the data set is segmented. If

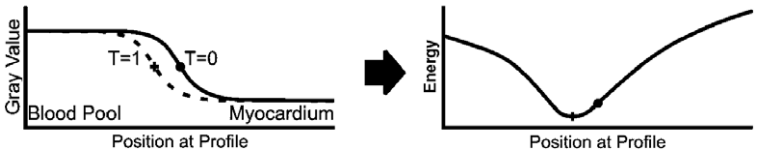

Fig. 1. Profiles from consecutive phases reveal a shift. The external energy distribution has a well-defined minimum at the location where the target ($T=1$) matches the reference ($T=0$) best.

necessary, the influence of noise can be reduced by applying a Gaussian filter on the profiles in the direction tangential to the contour [4].

3.3. Validation

The resulting contours were validated by calculating positioning errors in terms of average, RMS and maximum distance with respect to a golden standard. Distance calculations between discrete contours require a correct definition of chords between pairs of corresponding points along which distances are measured. To establish a so-called correspondence we use the Repeated Averaging Algorithm (RAA) [2], which defines chords perpendicular to an iteratively determined average contour.

Furthermore, we determined the influence of our algorithm on relevant physiological parameters, such as end-systolic volume (ESV), stroke volume (SV) and ejection fraction (EF). The required volumes were calculated by adding contour areas according to Simpson's rule.

4. Parameter optimization

The accuracy of our method depends on a number of parameters. To achieve accurate results an optimal parameter configuration for segmentation of short axis cardiac MR images was determined experimentally.

4.1. Data

The optimal parameter configuration was determined using a training set containing four cardiac MRI data sets. Each data set contained 75 short axis images from three slices, corresponding to approximately basal, mid and apical positions, and 25 phases. The data was obtained from two patients; scans were made before and after administering adenosine, to stimulate the heart cycle. The data was acquired using ECG gated cine MRI with a Philips Gyroscan Intera.

4.2. Golden standard for training set

Three experts segmented each data set in our training set twice. These six manual segmentations were averaged using the RAA, resulting in average contours, which reflect the common intentions of the experts. These average contours were considered to be the actual contour location and were therefore used as golden standard. The inter-observer variance for manual segmentation was determined in terms of positioning errors with respect to the golden standard. This resulted in RMS distances for the LV endocardium (1.1 ± 0.5 mm), LV epicardium (0.8 ± 0.3 mm) and RV endocardium (1.6 ± 0.9 mm). Furthermore it is important to note that the end systolic (ES) phase proved to be the most difficult to segment, exhibiting the largest inter-observer variation.

4.3. Experiment

The optimal parameter configuration was determined in an exhaustive search of the parameter space. Our method was tested by propagating all golden standard contours to the adjacent phase at each possible combination of parameter settings. The resulting contours were validated against the golden standard by calculating positioning errors. Such

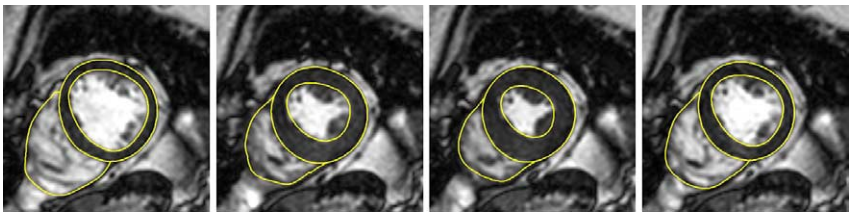

Fig. 2. Selected images from a short axis cardiac MR time sequence with propagated cardiac contours.

a so-called full factorial experiment generates a large, multidimensional parameter space filled with performance values. By applying Analysis of Variances (ANOVA) to this parameter space we determined the significant relations between parameters, consequently leading to the optimal parameter configuration.

4.4. Results

At the optimal parameter configuration, our method proved to be both fast and accurate. Fig. 2 shows an example of the results. The resulting contours of propagation from end diastole (ED), both forward and backward into time towards ES, were validated against the golden standard, again by calculating distance metrics, resulting in Fig. 3. The average positioning errors were within inter-user variation and pixel dimensions.

5. Validation

An elaborate validation was performed on a large number of clinical data sets. This validation included an evaluation of relevant physiological properties, next to determining positioning errors. Furthermore, our method was compared to a similar approach introduced by Spreeuwers and Breeuwer [3], which positions coupled active contours based on matching a single profile for both the LV endocardium and epicardium.

5.1. Data

Our test set contained 69 data sets, which included 9–14 contiguous slices and 15–50 phases. Consequently the number of images in the data sets varied (150–500). All images were 256×256 in size, covering a field of view ranging from 350×350 mm up to 480×480 mm. Only 11 data sets (16%) were continuous in time. In the other data sets, a number of phases from the repolarization phase of the heart cycle were missing.

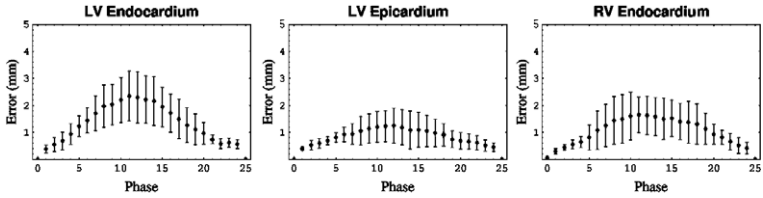

Fig. 3. Average RMS distance ± standard deviation between resulting contours and the golden standard over time.

Table 1
Average, RMS and maximum distances ± standard between the golden standard and the resulting contours from our method at end systole

Contours	Average distance (mm)	RMS distance (mm)	Maximum distance (mm)
LV endocardium	2.2 ± 1.1	2.6 ± 1.3	5.0 ± 1.7
LV epicardium	1.8 ± 1.0	2.3 ± 1.4	4.7 ± 3.6
RV endocardium	2.0 ± 1.2	2.6 ± 1.8	7.9 ± 8.1

5.2. Golden standard

Time considerations made the creation of a complete multiple user golden standard for 69 data sets not feasible. Therefore, the golden standard for these 69 data sets consisted of ED and ES manual segmentations only. The test set contained 753 time series, of which 511 were suitable for propagation and validation, i.e. all three cardiac contours were present at end diastole and end systole. A single cardiologist, who was not involved in generating the golden standard of the training set, generated the manual segmentations.

5.3. Experiment

All end diastolic contours were propagated towards end systole using our optimized method. The resulting ES contours were validated by calculating average, RMS and maximum positioning errors (see Table 1). The ESV, SV and EF were determined for all 69 data sets. We determined correlation coefficients and average errors ± standard deviation for the ESV (−0.8 ± 5.5 ml, R^2=0.98), SV (0.8 ± 5.5 ml, R^2=0.71) and EF (1.7 ± 6.8%, R^2=0.78), see Fig. 4. The resulting errors were small with respect to the errors made due to mispositioning of the apex (± 2 ml) or basal slice (± 10 ml).

5.4. Comparison

Repeating the experiment for the algorithm introduced by Spreeuwers and Breeuwer [3] resulted in positioning errors that are listed in Table 2. Furthermore, we determined the accuracy for the ESV (−2.3 ± 7.3 ml, R^2=0.96), SV (2.3 ± 7.3 ml, R^2=0.62) and EF (3.3 ± 8.6%, R^2=0.70). The contours resulting from our method were positioned

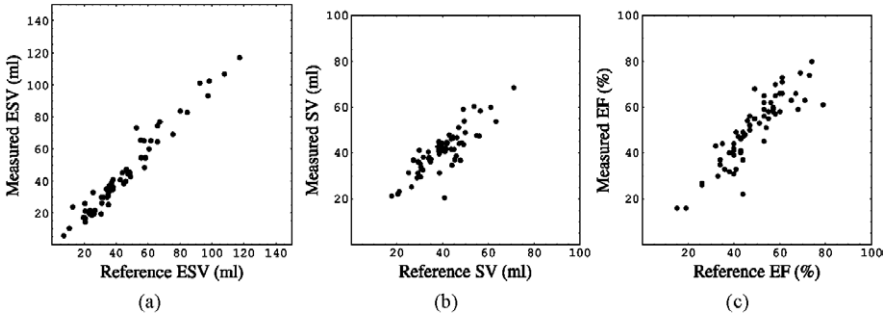

Fig. 4. Scatter plots from the ESV (a), SV (b) and EF (c).

Table 2
Average, RMS and maximum distances ± standard between the golden standard and the resulting contours from the contour propagation method from Spreeuwers and Breeuwer [3] at end systole

Contours	Average distance (mm)	RMS distance (mm)	Maximum distance (mm)
LV endocardium	2.6 ± 1.2	3.0 ± 1.3	5.7 ± 2.6
LV epicardium	2.1 ± 1.0	2.5 ± 1.2	5.1 ± 2.4

more accurately. Consequently, the estimated ESV, SV and EF were more accurate as well.

6. Conclusions

We have developed, optimized, technically evaluated and clinically validated a new cardiac contour propagation algorithm. The method has shown to be fast, robust and accurate. The resulting cardiac contours are positioned within the inter-observer manual segmentation range. The resulting contours can be used to accurately determine physiological parameters such as stroke volume and ejection fraction.

Acknowledgements

We are grateful to Eike Nagel from the Deutsches Herzzentrum Berlin and Luuk Spreeuwers and Evert-Jan Voncken from UMC Utrecht for supplying us with clinical image data.

References

[1] S. Lobregt, M.A. Viergever, A discrete dynamic contour model, IEEE Transactions on Medical Imaging 14 (1) (1995) 12–24.
[2] V. Chalana, Y. Kim, A methodology for evaluation of boundary detection algorithms on medical images, IEEE Transactions on Medical Imaging 16 (5) (1997) 642–652.
[3] L.J. Spreeuwers, M. Breeuwer, Detection of left ventricular Epi- and endocardial borders using coupled active contours, Proc. CARS2003, Computer Aided Radiology and Surgery, Number 1256 in International Congress Series, Elsevier Science B.V., 2003, pp. 1147–1152.
[4] S. Ho, G. Gerig, Scale-space on image profiles about an object boundary, Scale Space Methods in Computer Vision, Number 2695 in Lecture Notes in Computer Science, Springer, 2003, pp. 564–575.